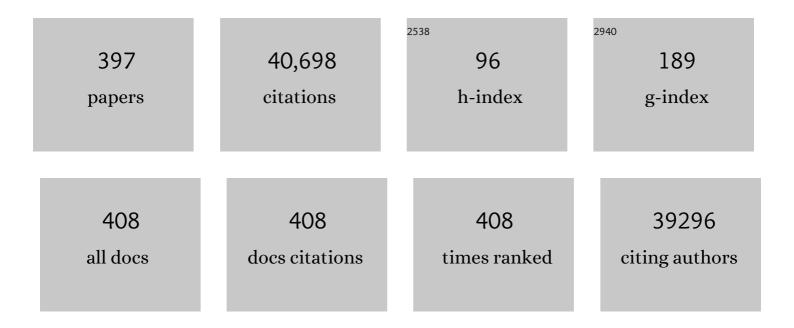
List of Publications by Year in descending order

Source: https://exaly.com/author-pdf/6108350/publications.pdf Version: 2024-02-01



SHUVAN SONG

#	Article	IF	CITATIONS
1	Intrinsic peroxidase-like activity of ferromagnetic nanoparticles. Nature Nanotechnology, 2007, 2, 577-583.	15.6	5,080
2	Noble metal-free hydrogen evolution catalysts for water splitting. Chemical Society Reviews, 2015, 44, 5148-5180.	18.7	4,776
3	Electrochemical Reduction of N ₂ under Ambient Conditions for Artificial N ₂ Fixation and Renewable Energy Storage Using N ₂ /NH ₃ Cycle. Advanced Materials, 2017, 29, 1604799.	11.1	969
4	Folded Structured Graphene Paper for High Performance Electrode Materials. Advanced Materials, 2012, 24, 1089-1094.	11.1	619
5	Industrial carbon dioxide capture and utilization: state of the art and future challenges. Chemical Society Reviews, 2020, 49, 8584-8686.	18.7	610
6	Singleâ€Crystalâ€toâ€Singleâ€Crystal Transformation of a Europium(III) Metal–Organic Framework Producing a Multiâ€responsive Luminescent Sensor. Advanced Functional Materials, 2014, 24, 4034-4041.	7.8	542
7	Formation of Onionâ€Like NiCo ₂ S ₄ Particles via Sequential Ionâ€Exchange for Hybrid Supercapacitors. Advanced Materials, 2017, 29, 1605051.	11.1	539
8	Proton-conducting crystalline porous materials. Chemical Society Reviews, 2017, 46, 464-480.	18.7	530
9	All-in-One Theranostic Nanoagent with Enhanced Reactive Oxygen Species Generation and Modulating Tumor Microenvironment Ability for Effective Tumor Eradication. ACS Nano, 2018, 12, 4886-4893.	7.3	510
10	Macroscopic Foamâ€Like Holey Ultrathin g ₃ N ₄ Nanosheets for Drastic Improvement of Visibleâ€Light Photocatalytic Activity. Advanced Energy Materials, 2016, 6, 1601273.	10.2	466
11	Ultrafast Formation of Amorphous Bimetallic Hydroxide Films on 3D Conductive Sulfide Nanoarrays for Largeâ€Currentâ€Density Oxygen Evolution Electrocatalysis. Advanced Materials, 2017, 29, 1700404.	11.1	462
12	Protective Coating of Superparamagnetic Iron Oxide Nanoparticles. Chemistry of Materials, 2003, 15, 1617-1627.	3.2	450
13	Hydrothermal synthetic strategies of inorganic semiconducting nanostructures. Chemical Society Reviews, 2013, 42, 5714.	18.7	437
14	Structural design of graphene for use in electrochemical energy storage devices. Chemical Society Reviews, 2015, 44, 6230-6257.	18.7	389
15	Corrosion engineering towards efficient oxygen evolution electrodes with stable catalytic activity for over 6000 hours. Nature Communications, 2018, 9, 2609.	5.8	389
16	Metal–Organic Framework Hybridâ€Assisted Formation of Co ₃ O ₄ /Coâ€Fe Oxide Doubleâ€Shelled Nanoboxes for Enhanced Oxygen Evolution. Advanced Materials, 2018, 30, e1801211.	11.1	374
17	Multi-shelled metal oxides prepared via an anion-adsorption mechanism for lithium-ion batteries. Nature Energy, 2016, 1, .	19.8	352
18	Coupling Subâ€Nanometric Copper Clusters with Quasiâ€Amorphous Cobalt Sulfide Yields Efficient and Robust Electrocatalysts for Water Splitting Reaction. Advanced Materials, 2017, 29, 1606200.	11.1	350

#	Article	IF	CITATIONS
19	Graphene oxide covalently grafted upconversion nanoparticles for combined NIR mediated imaging and photothermal/photodynamic cancer therapy. Biomaterials, 2013, 34, 7715-7724.	5.7	344
20	One-dimensional channel-structured Eu-MOF for sensing small organic molecules and Cu2+ ion. Journal of Materials Chemistry A, 2013, 1, 11043.	5.2	341
21	Homogeneous CoO on Graphene for Binderâ€Free and Ultralongâ€Life Lithium Ion Batteries. Advanced Functional Materials, 2013, 23, 4345-4353.	7.8	333
22	Pt@CeO ₂ Multicore@Shell Self-Assembled Nanospheres: Clean Synthesis, Structure Optimization, and Catalytic Applications. Journal of the American Chemical Society, 2013, 135, 15864-15872.	6.6	323
23	Oneâ€Dimensional Fe ₂ P Acts as a Fenton Agent in Response to NIRâ€Il Light and Ultrasound for Deep Tumor Synergetic Theranostics. Angewandte Chemie - International Edition, 2019, 58, 2407-2412.	7.2	315
24	Binary temporal upconversion codes of Mn2+-activated nanoparticles for multilevel anti-counterfeiting. Nature Communications, 2017, 8, 899.	5.8	290
25	Synthesis of 3D Hierarchical Fe ₃ O ₄ /Graphene Composites with High Lithium Storage Capacity and for Controlled Drug Delivery. Journal of Physical Chemistry C, 2011, 115, 21567-21573.	1.5	288
26	Highly efficient heterogeneous catalytic materials derived from metal-organic framework supports/precursors. Coordination Chemistry Reviews, 2017, 337, 80-96.	9.5	282
27	Ultrathin Porous NiFeV Ternary Layer Hydroxide Nanosheets as a Highly Efficient Bifunctional Electrocatalyst for Overall Water Splitting. Small, 2018, 14, 1703257.	5.2	279
28	Bismuthene for highly efficient carbon dioxide electroreduction reaction. Nature Communications, 2020, 11, 1088.	5.8	278
29	In Situ Generation of Bifunctional, Efficient Fe-Based Catalysts from Mackinawite Iron Sulfide for Water Splitting. CheM, 2018, 4, 1139-1152.	5.8	271
30	Prevention of dendrite growth and volume expansion to give high-performance aprotic bimetallic Li-Na alloy–O2 batteries. Nature Chemistry, 2019, 11, 64-70.	6.6	265
31	Lanthanide Ion Codoped Emitters for Tailoring Emission Trajectory and Temperature Sensing. Advanced Functional Materials, 2015, 25, 1463-1469.	7.8	263
32	Studies on the magnetism of cobalt ferrite nanocrystals synthesized by hydrothermal method. Journal of Solid State Chemistry, 2008, 181, 245-252.	1.4	260
33	Cathode Surfaceâ€Induced, Solvationâ€Mediated, Micrometerâ€Sized Li ₂ O ₂ Cycling for Li–O ₂ Batteries. Advanced Materials, 2016, 28, 9620-9628.	11.1	232
34	Surfactantâ€Free Aqueous Synthesis of Pure Singleâ€Crystalline SnSe Nanosheet Clusters as Anode for High Energy―and Powerâ€Density Sodiumâ€Ion Batteries. Advanced Materials, 2017, 29, 1602469.	11.1	231
35	Rhodium–nickel nanoparticles grown on graphene as highly efficient catalyst for complete decomposition of hydrous hydrazine at room temperature for chemical hydrogen storage. Energy and Environmental Science, 2012, 5, 6885.	15.6	214
36	Synthesis, characterization and assembly of BiOCl nanostructure and their photocatalytic properties. CrystEngComm, 2009, 11, 1857.	1.3	210

#	Article	IF	CITATIONS
37	Remote manipulation of upconversion luminescence. Chemical Society Reviews, 2018, 47, 6473-6485.	18.7	210
38	Ultrafast Synthesis of Ultrasmall Poly(Vinylpyrrolidone)â€Protected Bismuth Nanodots as a Multifunctional Theranostic Agent for In Vivo Dualâ€Modal CT/Photothermalâ€Imagingâ€Guided Photothermal Therapy. Advanced Functional Materials, 2017, 27, 1702018.	7.8	203
39	Facile Synthesis and Assemblies of Flowerlike SnS ₂ and In ³⁺ -Doped SnS ₂ : Hierarchical Structures and Their Enhanced Photocatalytic Property. Journal of Physical Chemistry C, 2009, 113, 1280-1285.	1.5	201
40	Crystallization design of MnO2 towards better supercapacitance. CrystEngComm, 2012, 14, 5892.	1.3	187
41	Copper(I) Phosphide Nanocrystals for In Situ Selfâ€Generation Magnetic Resonance Imagingâ€Guided Photothermalâ€Enhanced Chemodynamic Synergetic Therapy Resisting Deepâ€Seated Tumor. Advanced Functional Materials, 2019, 29, 1904678.	7.8	185
42	Bottom-up engineering of thermoelectric nanomaterials and devices from solution-processed nanoparticle building blocks. Chemical Society Reviews, 2017, 46, 3510-3528.	18.7	184
43	Alkali Metal Anodes for Rechargeable Batteries. CheM, 2019, 5, 313-338.	5.8	170
44	Room temperature, template-free synthesis of BiOI hierarchical structures: Visible-light photocatalytic and electrochemical hydrogen storage properties. Dalton Transactions, 2010, 39, 3273.	1.6	169
45	Preparation and enhanced visible light photocatalytic activity of novel g-C ₃ N ₄ nanosheets loaded with Ag ₂ CO ₃ nanoparticles. Nanoscale, 2015, 7, 758-764.	2.8	166
46	Hydrothermal Synthesis and Thermoelectric Transport Properties of Impurityâ€Free Antimony Telluride Hexagonal Nanoplates. Advanced Materials, 2008, 20, 1892-1897.	11.1	162
47	Flexible Electrodes for Sodiumâ€lon Batteries: Recent Progress and Perspectives. Advanced Materials, 2017, 29, 1703012.	11.1	156
48	Two Coordination Polymers of Ag(I) with 5-Sulfosalicylic Acid. Crystal Growth and Design, 2005, 5, 807-812.	1.4	155
49	A Metal–Organic Framework/DNA Hybrid System as a Novel Fluorescent Biosensor for Mercury(II) Ion Detection. Chemistry - A European Journal, 2016, 22, 477-480.	1.7	155
50	Morphology-Controlled Synthesis of Magnetites with Nanoporous Structures and Excellent Magnetic Properties. Chemistry of Materials, 2008, 20, 198-204.	3.2	152
51	Influence of Neutral Ligands on the Structures of Silver(I) Sulfonates. Inorganic Chemistry, 2005, 44, 9374-9383.	1.9	151
52	A europium(<scp>iii</scp>) based metal–organic framework: bifunctional properties related to sensing and electronic conductivity. Journal of Materials Chemistry A, 2014, 2, 237-244.	5.2	149
53	Pt/CeO ₂ @MOF Core@Shell Nanoreactor for Selective Hydrogenation of Furfural via the Channel Screening Effect. ACS Catalysis, 2018, 8, 8506-8512.	5.5	145
54	Preparation of Carbonâ€Rich <i>g</i> ₃ N ₄ Nanosheets with Enhanced Visible Light Utilization for Efficient Photocatalytic Hydrogen Production. Small, 2017, 13, 1701552.	5.2	142

#	Article	IF	CITATIONS
55	A Flexible and Wearable Lithium–Oxygen Battery with Record Energy Density achieved by the Interlaced Architecture inspired by Bamboo Slips. Advanced Materials, 2016, 28, 8413-8418.	11.1	138
56	In Situ Formation of Co ₉ S ₈ Quantum Dots in MOFâ€Đerived Ternary Metal Layered Double Hydroxide Nanoarrays for Highâ€Performance Hybrid Supercapacitors. Advanced Energy Materials, 2020, 10, 1903193.	10.2	138
57	In situ loading of Ag2WO4 on ultrathin g-C3N4 nanosheets with highly enhanced photocatalytic performance. Journal of Hazardous Materials, 2016, 313, 219-228.	6.5	135
58	Two-dimensional NiCo ₂ O ₄ nanosheet-coated three-dimensional graphene networks for high-rate, long-cycle-life supercapacitors. Nanoscale, 2015, 7, 7035-7039.	2.8	134
59	Na ₂ S ₂ O ₈ Nanoparticles Trigger Antitumor Immunotherapy through Reactive Oxygen Species Storm and Surge of Tumor Osmolarity. Journal of the American Chemical Society, 2020, 142, 21751-21757.	6.6	133
60	Green synthesis of Pt/CeO2/graphene hybrid nanomaterials with remarkably enhanced electrocatalytic properties. Chemical Communications, 2012, 48, 2885.	2.2	131
61	ZnOâ€Functionalized Upconverting Nanotheranostic Agent: Multiâ€Modality Imagingâ€Guided Chemotherapy with Onâ€Demand Drug Release Triggered by pH. Angewandte Chemie - International Edition, 2015, 54, 536-540.	7.2	131
62	Controllable Synthesis of Mesoporous TiO ₂ Polymorphs with Tunable Crystal Structure for Enhanced Photocatalytic H ₂ Production. Advanced Energy Materials, 2019, 9, 1901634.	10.2	131
63	Syntheses, Structures, and Photoluminescent Properties of 12 New Metal–Organic Frameworks Constructed by a Flexible Dicarboxylate and Various N-Donor Ligands. Crystal Growth and Design, 2012, 12, 2397-2410.	1.4	129
64	Molecular Engineering of Monodisperse SnO ₂ Nanocrystals Anchored on Doped Graphene with Highâ€Performance Lithium/Sodiumâ€Storage Properties in Half/Full Cells. Advanced Energy Materials, 2019, 9, 1802993.	10.2	129
65	Selectively Deposited Noble Metal Nanoparticles on Fe ₃ O ₄ /Graphene Composites: Stable, Recyclable, and Magnetically Separable Catalysts. Chemistry - A European Journal, 2012, 18, 7601-7607.	1.7	126
66	Luminescent Anionic Metal–Organic Framework with Potential Nitrobenzene Sensing. Crystal Growth and Design, 2014, 14, 3174-3178.	1.4	126
67	Bi2Te3 nanoplates and nanoflowers: Synthesized by hydrothermal process and their enhanced thermoelectric properties. CrystEngComm, 2012, 14, 2159.	1.3	125
68	Syntheses and Applications of Noble-Metal-free CeO2-Based Mixed-Oxide Nanocatalysts. CheM, 2019, 5, 1743-1774.	5.8	125
69	Defect modified zinc oxide with augmenting sonodynamic reactive oxygen species generation. Biomaterials, 2020, 251, 120075.	5.7	125
70	Encapsulation of Ln ^{III} lons/Dyes within a Microporous Anionic MOF by Postâ€synthetic Ionic Exchange Serving as a Ln ^{III} Ion Probe and Twoâ€Color Luminescent Sensors. Chemistry - A European Journal, 2015, 21, 9748-9752.	1.7	123
71	Formation of Septupleâ€Shelled (Co _{2/3} Mn _{1/3})(Co _{5/6} Mn _{1/6}) ₂ O ₄ Hollow Spheres as Electrode Material for Alkaline Rechargeable Battery. Advanced Materials, 2017, 29, 1700550.	11.1	122
72	Nanoconfined nitrogen-doped carbon-coated MnO nanoparticles in graphene enabling high performance for lithium-ion batteries and oxygen reduction reaction. Chemical Science, 2016, 7, 4284-4290.	3.7	121

#	Article	IF	CITATIONS
73	Multishelled Ni <i> _x </i> Co ₃₋ <i> _x </i> O ₄ Hollow Microspheres Derived from Bimetal-Organic Frameworks as Anode Materials for High-Performance Lithium-Ion Batteries. Small, 2017, 13, 1604270.	5.2	120
74	A new type of double-chain based 3D lanthanide(iii) metal–organic framework demonstrating proton conduction and tunable emission. Chemical Communications, 2014, 50, 1912.	2.2	118
75	Polydopamine coated manganese oxide nanoparticles with ultrahigh relaxivity as nanotheranostic agents for magnetic resonance imaging guided synergetic chemo-/photothermal therapy. Chemical Science, 2016, 7, 6695-6700.	3.7	116
76	Hydrothermal Synthesis and High Photocatalytic Activity of 3D Wurtzite ZnSe Hierarchical Nanostructures. Journal of Physical Chemistry C, 2008, 112, 17095-17101.	1.5	115
77	Co ₉ S ₈ Nanoparticlesâ€Embedded N/Sâ€Codoped Carbon Nanofibers Derived from Metal–Organic Frameworkâ€Wrapped CdS Nanowires for Efficient Oxygen Evolution Reaction. Small, 2018, 14, e1704035.	5.2	115
78	α-NaYb(Mn)F ₄ :Er ³⁺ /Tm ³⁺ @NaYF ₄ UCNPs as "Band-Shape―Luminescent Nanothermometers over a Wide Temperature Range. ACS Applied Materials & Interfaces, 2015, 7, 20813-20819.	4.0	114
79	Catalytic Mechanisms of Nanozymes and Their Applications in Biomedicine. Bioconjugate Chemistry, 2019, 30, 1273-1296.	1.8	113
80	Surface photovoltage characterization of a ZnO nanowire array/CdS quantum dot heterogeneous film and its application for photovoltaic devices. Nanotechnology, 2009, 20, 155707.	1.3	110
81	Smart Porous Core–Shell Cuprous Oxide Nanocatalyst with High Biocompatibility for Acidâ€Triggered Chemo/Chemodynamic Synergistic Therapy. Small, 2020, 16, e2001805.	5.2	109
82	Bloodâ€Capillaryâ€Inspired, Freeâ€Standing, Flexible, and Lowâ€Cost Superâ€Hydrophobic Nâ€CNTs@SS Catho for Highâ€Capacity, Highâ€Rate, and Stable Liâ€Air Batteries. Advanced Energy Materials, 2018, 8, 1702242.	des 10.2	108
83	Metal–organic framework-based materials for the recovery of uranium from aqueous solutions. Inorganic Chemistry Frontiers, 2019, 6, 1924-1937.	3.0	108
84	A "Solid Dualâ€lonsâ€Transformation―Route to S,N Coâ€Doped Carbon Nanotubes as Highly Efficient "Metalâ€Free―Catalysts for Organic Reactions. Advanced Materials, 2016, 28, 10679-10683.	11.1	107
85	Acid–Baseâ€Triggered Structural Transformation of a Polyoxometalate Core Inside a Dodecahedraneâ€like Silver Thiolate Shell. Angewandte Chemie - International Edition, 2016, 55, 3699-3703.	7.2	106
86	Preparation and enhanced photocatalytic performance of sulfur doped terminal-methylated g-C ₃ N ₄ nanosheets with extended visible-light response. Journal of Materials Chemistry A, 2019, 7, 20640-20648.	5.2	105
87	Plasmonic Pt Superstructures with Boosted Nearâ€Infrared Absorption and Photothermal Conversion Efficiency in the Second Biowindow for Cancer Therapy. Advanced Materials, 2019, 31, e1904836.	11.1	105
88	Synthesis of highly active Pt–CeO2 hybrids with tunable secondary nanostructures for the catalytic hydrolysis of ammonia borane. Chemical Communications, 2012, 48, 10207.	2.2	104
89	3D Fe3S4 flower-like microspheres: high-yield synthesis via a biomolecule-assisted solution approach, their electrical, magnetic and electrochemical hydrogen storage properties. Dalton Transactions, 2009, , 9246.	1.6	102
90	Hydrothermal Synthesis, Structures, and Luminescent Properties of Seven d10 Metalâ^'Organic Frameworks Based on 9,9-Dipropylfluorene-2,7-Dicarboxylic Acid (H2DFDA). Crystal Growth and Design, 2009, 9, 1394-1401.	1.4	101

#	Article	IF	CITATIONS
91	In situ generated FeF 3 in homogeneous iron matrix toward high-performance cathode material for sodium-ion batteries. Nano Energy, 2014, 10, 295-304.	8.2	101
92	CeO2-encapsulated noble metal nanocatalysts: enhanced activity and stability for catalytic application. NPG Asia Materials, 2015, 7, e179-e179.	3.8	101
93	Lanthanide Anionic Metal–Organic Frameworks Containing Semirigid Tetracarboxylate Ligands: Structure, Photoluminescence, and Magnetism. Crystal Growth and Design, 2012, 12, 1808-1815.	1.4	100
94	Stimuli-responsive nanotheranostics based on lanthanide-doped upconversion nanoparticles for cancer imaging and therapy: current advances and future challenges. Nano Today, 2019, 25, 38-67.	6.2	100
95	Syntheses, Structures, and Characterizations of Four New Silver(I) Sulfonate Coordination Polymers with Neutral Ligands. Crystal Growth and Design, 2006, 6, 209-215.	1.4	99
96	Microwave-assisted synthesis of BiOBr/graphene nanocomposites and their enhanced photocatalytic activity. Dalton Transactions, 2012, 41, 10472.	1.6	96
97	A tetranuclear copper cluster-based MOF with sulfonate–carboxylate ligands exhibiting high proton conduction properties. Chemical Communications, 2015, 51, 8150-8152.	2.2	96
98	Copper Salts Mediated Morphological Transformation of Cu2O from Cubes to Hierarchical Flower-like or Microspheres and Their Supercapacitors Performances. Scientific Reports, 2015, 5, 9672.	1.6	90
99	Rectangular AgIn(WO ₄) ₂ Nanotubes: A Promising Photoelectric Material. Advanced Functional Materials, 2008, 18, 2328-2334.	7.8	88
100	Vapor-phase crystallization route to oxidized Cu foils in air as anode materials for lithium-ion batteries. CrystEngComm, 2013, 15, 144-151.	1.3	87
101	Hollow Multishelled Structure of Heterogeneous Co ₃ O ₄ –CeO _{2â^'} <i>_x</i> Nanocomposite for CO Catalytic Oxidation. Advanced Functional Materials, 2019, 29, 1806588.	7.8	86
102	Syntheses, Structures, and Photoluminescent Properties of Coordination Polymers Based on 1,4-Bis(imidazol-l-yl-methyl)benzene and Various Aromatic Dicarboxylic Acids. Crystal Growth and Design, 2012, 12, 253-263.	1.4	84
103	A Temperatureâ€Responsive Smart Europium Metalâ€Organic Framework Switch for Reversible Capture and Release of Intrinsic Eu ³⁺ lons. Advanced Science, 2015, 2, 1500012.	5.6	83
104	Bimetallic NiCo2S4 Nanoneedles Anchored on Mesocarbon Microbeads as Advanced Electrodes for Asymmetric Supercapacitors. Nano-Micro Letters, 2019, 11, 35.	14.4	83
105	Prussian Blue Analogs and Their Derived Nanomaterials for Electrochemical Energy Storage and Electrocatalysis. Small Methods, 2021, 5, e2001000.	4.6	81
106	Hierarchically structured Fe ₃ O ₄ microspheres: morphology control and their application in wastewater treatment. CrystEngComm, 2011, 13, 642-648.	1.3	80
107	Facile Synthesis and Properties of Hierarchical Double-Walled Copper Silicate Hollow Nanofibers Assembled by Nanotubes. ACS Nano, 2014, 8, 3664-3670.	7.3	80
108	Dualâ€Defects Adjusted Crystalâ€Field Splitting of LaCo _{1â^'<i>x</i>} Ni _{<i>x</i>} O _{3â^'<i>Î′</i>} Hollow Multishelled Structures for Efficient Oxygen Evolution. Angewandte Chemie - International Edition, 2020, 59, 19691-19695.	7.2	80

SHUYAN SONG

#	Article	IF	CITATIONS
109	Novel Multifunctional Nanocomposites: Magnetic Mesoporous Silica Nanospheres Covalently Bonded with Near-Infrared Luminescent Lanthanide Complexes. Langmuir, 2010, 26, 3596-3600.	1.6	78
110	Yb ³⁺ /Er ³⁺ -Codoped Bi ₂ O ₃ Nanospheres: Probe for Upconversion Luminescence Imaging and Binary Contrast Agent for Computed Tomography Imaging. ACS Applied Materials & Interfaces, 2015, 7, 26346-26354.	4.0	78
111	A Bipolar and Selfâ€Polymerized Phthalocyanine Complex for Fast and Tunable Energy Storage in Dual″on Batteries. Angewandte Chemie - International Edition, 2019, 58, 10204-10208.	7.2	78
112	Fe ₃ O ₄ @SiO ₂ @TiO ₂ @Pt Hierarchical Core–Shell Microspheres: Controlled Synthesis, Enhanced Degradation System, and Rapid Magnetic Separation to Recycle. Crystal Growth and Design, 2014, 14, 5506-5511.	1.4	77
113	Preparation and gas storage of high surface area microporous carbon derived from biomass source cornstalks. Bioresource Technology, 2008, 99, 4803-4808.	4.8	76
114	A stable, pillar-layer metal–organic framework containing uncoordinated carboxyl groups for separation of transition metal ions. Chemical Communications, 2014, 50, 6406-6408.	2.2	76
115	One-pot synthesis of flowerlike Ni7S6and its application in selective hydrogenation of chloronitrobenzene. Journal of Materials Chemistry, 2010, 20, 1078-1085.	6.7	75
116	Co ₃ O ₄ @CeO ₂ Core@Shell Cubes: Designed Synthesis and Optimization of Catalytic Properties. Chemistry - A European Journal, 2014, 20, 4469-4473.	1.7	75
117	Photothermal-Enhanced Inactivation of Clutathione Peroxidase for Ferroptosis Sensitized by an Autophagy Promotor. ACS Applied Materials & Interfaces, 2019, 11, 42988-42997.	4.0	75
118	Copper doped ceria porous nanostructures towards a highly efficient bifunctional catalyst for carbon monoxide and nitric oxide elimination. Chemical Science, 2015, 6, 2495-2500.	3.7	74
119	CeO ₂ nanowires self-inserted into porous Co ₃ O ₄ frameworks as high-performance "noble metal free―hetero-catalysts. Chemical Science, 2016, 7, 1109-1114.	3.7	74
120	Achieving the Tradeâ€Off between Selectivity and Activity in Semihydrogenation of Alkynes by Fabrication of (Asymmetrical Pd@Ag Core)@(CeO ₂ Shell) Nanocatalysts via Autoredox Reaction. Advanced Materials, 2017, 29, 1605332.	11.1	73
121	Optimization of Bi ³⁺ in Upconversion Nanoparticles Induced Simultaneous Enhancement of Near-Infrared Optical and X-ray Computed Tomography Imaging Capability. ACS Applied Materials & amp; Interfaces, 2016, 8, 27490-27497.	4.0	72
122	Highâ€Performance Integrated Selfâ€Package Flexible Li–O ₂ Battery Based on Stable Composite Anode and Flexible Gas Diffusion Layer. Advanced Materials, 2017, 29, 1700378.	11.1	72
123	Confining the Nucleation of Pt to In Situ Form (Ptâ€Enriched Cage)@CeO ₂ Core@Shell Nanostructure as Excellent Catalysts for Hydrogenation Reactions. Advanced Materials, 2017, 29, 1700495.	11.1	72
124	Design strategies and applications of charged metal organic frameworks. Coordination Chemistry Reviews, 2019, 398, 113007.	9.5	72
125	Surface Sulfurization of NiCo-Layered Double Hydroxide Nanosheets Enable Superior and Durable Oxygen Evolution Electrocatalysis. ACS Applied Energy Materials, 2018, 1, 4040-4049.	2.5	71
126	Highly transparent bulk PMMA/ZnO nanocomposites with bright visible luminescence and efficient UV-shielding capability. Journal of Materials Chemistry, 2012, 22, 11971.	6.7	70

#	Article	IF	CITATIONS
127	Water-soluble inorganic salts with ultrahigh specific capacitance: crystallization transformation investigation of CuCl2 electrodes. CrystEngComm, 2013, 15, 10367.	1.3	70
128	An active-site-accessible porous metal–organic framework composed of triangular building units: preparation, catalytic activity and magnetic property. Chemical Communications, 2012, 48, 11118.	2.2	69
129	Faceted Cu ₂ O structures with enhanced Li-ion battery anode performances. CrystEngComm, 2015, 17, 2110-2117.	1.3	69
130	Beyond graphene: materials chemistry toward high performance inorganic functional materials. Journal of Materials Chemistry A, 2015, 3, 2441-2453.	5.2	69
131	Multifunctional core/satellite polydopamine@Nd3+-sensitized upconversion nanocomposite: A single 808 nm near-infrared light-triggered theranostic platform for in vivo imaging-guided photothermal therapy. Nano Research, 2017, 10, 3434-3446.	5.8	69
132	Direct hydrothermal synthesis of single-crystalline triangular Fe3O4 nanoprisms. CrystEngComm, 2010, 12, 2060.	1.3	68
133	Multifunctional Cu–Ag ₂ S nanoparticles with high photothermal conversion efficiency for photoacoustic imaging-guided photothermal therapy <i>in vivo</i> . Nanoscale, 2018, 10, 825-831.	2.8	68
134	Synthesis and Optical Properties of Europiumâ€Complexâ€Doped Inorganic/Organic Hybrid Materials Built from Oxo–Hydroxo Organotin Nano Building Blocks. Chemistry - A European Journal, 2010, 16, 1903-1910.	1.7	67
135	Microwaveâ€Assisted Modular Fabrication of Nanoscale Luminescent Metalâ€Organic Framework for Molecular Sensing. ChemPhysChem, 2012, 13, 2734-2738.	1.0	67
136	A multifunctional proton-conducting and sensing pillar-layer framework based on [24-MC-6] heterometallic crown clusters. Chemical Communications, 2013, 49, 8483.	2.2	67
137	Lanthanide doped Bi ₂ O ₃ upconversion luminescence nanospheres for temperature sensing and optical imaging. Dalton Transactions, 2016, 45, 2686-2693.	1.6	67
138	Structural Study of Silver(I) Sulfonate Complexes with Pyrazine Derivatives. Inorganic Chemistry, 2007, 46, 7299-7311.	1.9	65
139	Tunnel-dependent supercapacitance of MnO ₂ : effects of crystal structure. Journal of Applied Crystallography, 2013, 46, 1128-1135.	1.9	65
140	Green and controlled synthesis of Cu2O–graphene hierarchical nanohybrids as high-performance anode materials for lithium-ion batteries via an ultrasound assisted approach. Dalton Transactions, 2012, 41, 4316.	1.6	64
141	Energy Migration Upconversion in Manganese(II)â€Đoped Nanoparticles. Angewandte Chemie - International Edition, 2015, 54, 13312-13317.	7.2	64
142	Double Switch Biodegradable Porous Hollow Trinickel Monophosphide Nanospheres for Multimodal Imaging Guided Photothermal Therapy. Nano Letters, 2019, 19, 5093-5101.	4.5	64
143	Unraveling the physical chemistry and materials science of CeO2-based nanostructures. CheM, 2021, 7, 2022-2059.	5.8	64
144	A Eu/Tb-codoped coordination polymer luminescent thermometer. Inorganic Chemistry Frontiers, 2014, 1, 757-760.	3.0	63

#	Article	IF	CITATIONS
145	<scp>l</scp> â€Arginineâ€Triggered Selfâ€Assembly of CeO ₂ Nanosheaths on Palladium Nanoparticles in Water. Angewandte Chemie - International Edition, 2016, 55, 4542-4546.	7.2	63
146	Rhâ€Niâ€B Nanoparticles as Highly Efficient Catalysts for Hydrogen Generation from Hydrous Hydrazine. Advanced Energy Materials, 2015, 5, 1401879.	10.2	61
147	A Porphyrinâ€Based Porous <i>rtl</i> Metal–Organic Framework as an Efficient Catalyst for the Cycloaddition of CO ₂ to Epoxides. Chemistry - A European Journal, 2016, 22, 16991-16997.	1.7	61
148	Porous Co3O4 microcubes: hydrothermal synthesis, catalytic and magnetic properties. CrystEngComm, 2011, 13, 2123.	1.3	60
149	A Controllable Surface Etching Strategy for Wellâ€Defined Spiny Yolk@Shell CuO@CeO ₂ Cubes and Their Catalytic Performance Boost. Advanced Functional Materials, 2018, 28, 1802559.	7.8	60
150	Syntheses, structures and physical properties of transition metal–organic frameworks assembled from trigonal heterofunctional ligands. Dalton Transactions, 2012, 41, 10412.	1.6	58
151	Syntheses, crystal structures, visible and near-IR luminescent properties of ternary lanthanide (Dy3+,) Tj ETQq1 1 of Luminescence, 2008, 128, 1957-1964.	0.78431 1.5	4 rgBT /Over 57
152	Near-infrared luminescent xerogel materials covalently bonded with ternary lanthanide [Er(iii), Nd(iii), Yb(iii), Sm(iii)] complexes. Dalton Transactions, 2009, , 2406.	1.6	57
153	Comparative Study of Structural Changes in NH ₃ BH ₃ , LiNH ₂ BH ₃ , and KNH ₂ BH ₃ During Dehydrogenation Process. Journal of Physical Chemistry C, 2012, 116, 5957-5964.	1.5	57
154	An ionic aqueous pseudocapacitor system: electroactive ions in both a salt electrode and redox electrolyte. RSC Advances, 2014, 4, 23338.	1.7	57
155	Mesoporous TiO ₂ -Based Photoanode Sensitized by BiOI and Investigation of Its Photovoltaic Behavior. Langmuir, 2015, 31, 10279-10284.	1.6	57
156	Investigating the Hybridâ€&tructureâ€Effect of CeO ₂ â€Encapsulated Au Nanostructures on the Transfer Coupling of Nitrobenzene. Advanced Materials, 2018, 30, 1704416.	11.1	57
157	A ratiometric fluorescent sensor with dual response of Fe3+/Cu2+ based on europium post-modified sulfone-metal-organic frameworks and its logical application. Talanta, 2019, 197, 291-298.	2.9	57
158	Highâ€Performance Ultrathin Co ₃ O ₄ Nanosheet Supported PdO/CeO ₂ Catalysts for Methane Combustion. Advanced Energy Materials, 2019, 9, 1803583.	10.2	57
159	Growth of lanthanide-doped LiGdF4 nanoparticles induced by LiLuF4 core as tri-modal imaging bioprobes. Biomaterials, 2015, 65, 115-123.	5.7	55
160	Rare earth fluorides upconversion nanophosphors: from synthesis to applications in bioimaging. CrystEngComm, 2013, 15, 7142.	1.3	54
161	Fabrication of TiO ₂ –BiOCl double-layer nanostructure arrays for photoelectrochemical water splitting. CrystEngComm, 2014, 16, 820-825.	1.3	54
162	Hydrothermal synthesis and photoluminescent properties of stacked indium sulfide superstructures. Chemical Communications, 2008, , 1476.	2.2	53

#	Article	IF	CITATIONS
163	A study on the near-infrared luminescent properties of xerogel materials doped with dysprosium complexes. Dalton Transactions, 2009, , 6593.	1.6	53
164	Assembly of three coordination polymers based on a sulfonic–carboxylic ligand showing high proton conductivity. Dalton Transactions, 2015, 44, 948-954.	1.6	53
165	Superior electrode performance of mesoporous hollow TiO2 microspheres through efficient hierarchical nanostructures. Journal of Power Sources, 2011, 196, 8618-8624.	4.0	52
166	A Series of Metal–Organic Frameworks Constructed From a V-shaped Tripodal Carboxylate Ligand: Syntheses, Structures, Photoluminescent, and Magnetic Properties. Crystal Growth and Design, 2013, 13, 2756-2765.	1.4	52
167	CRYSTALLIZATION OF OXIDES AS FUNCTIONAL MATERIALS. Functional Materials Letters, 2012, 05, 1230002.	0.7	51
168	Decoration of Pt on Cu/Co double-doped CeO ₂ nanospheres and their greatly enhanced catalytic activity. Chemical Science, 2016, 7, 1867-1873.	3.7	51
169	Microporous carbon derived from pinecone hull as anode material for lithium secondary batteries. Materials Letters, 2007, 61, 5209-5212.	1.3	50
170	Graphene Oxide Induced Formation of Pt–CeO ₂ Hybrid Nanoflowers with Tunable CeO ₂ Thickness for Catalytic Hydrolysis of Ammonia Borane. Chemistry - A European Journal, 2013, 19, 8082-8086.	1.7	50
171	Insights into high CO-SCR performance of CuCoAlO catalysts derived from LDH/MOFs composites and study of H2O/SO2 and alkali metal resistance. Chemical Engineering Journal, 2021, 426, 131873.	6.6	50
172	Boosting Chemodynamic Therapy by the Synergistic Effect of Co-Catalyze and Photothermal Effect Triggered by the Second Near-Infrared Light. Nano-Micro Letters, 2020, 12, 180.	14.4	49
173	Selected-Control Synthesis of Metal Phosphonate Nanoparticles and Nanorods. Inorganic Chemistry, 2005, 44, 2140-2142.	1.9	48
174	Solid state NMR study on the thermal decomposition pathway of sodium amidoborane NaNH2BH3. Journal of Materials Chemistry, 2011, 21, 2609.	6.7	48
175	Ballâ€Milling Induced Debonding of Surface Atoms from Metal Bulk for Construing Highâ€Performance Dual‧ite Singleâ€Atom Catalysts. Angewandte Chemie - International Edition, 2021, 60, 23154-23158.	7.2	48
176	Stabilization of Imidosamarium(III) Cubane by Amidinates. Inorganic Chemistry, 2009, 48, 6344-6346.	1.9	47
177	Syntheses, structures, photoluminescence, and magnetic properties of (3,6)- and 4-connected lanthanide metal–organic frameworks with a semirigid tricarboxylate ligand. Dalton Transactions, 2012, 41, 4772.	1.6	47
178	Polymorphic crystallization of Cu ₂ O compound. CrystEngComm, 2014, 16, 5257-5267.	1.3	47
179	Water crystallization to create ice spacers between graphene oxide sheets for highly electroactive graphene paper. CrystEngComm, 2014, 16, 7771.	1.3	47
180	MOF/PCP-based Electrocatalysts for the Oxygen Reduction Reaction. Electrochemical Energy Reviews, 2022, 5, 32-81.	13.1	47

#	Article	IF	CITATIONS
181	Microemulsion-mediated solvothermal synthesis and photoluminescent property of 3D flowerlike MnWO4 micro/nanocomposite structure. Solid State Sciences, 2008, 10, 1299-1304.	1.5	46
182	Highly thermostable lanthanide metal–organic frameworks exhibiting unique selectivity for nitro explosives. RSC Advances, 2015, 5, 93-98.	1.7	46
183	Reduced graphene oxide nanosheet modified NiMn-LDH nanoflake arrays for high-performance supercapacitors. Chemical Communications, 2018, 54, 10172-10175.	2.2	46
184	Recent Advances in Graphitic Carbon Nitride Supported Singleâ€Atom Catalysts for Energy Conversion. ChemCatChem, 2021, 13, 1250-1270.	1.8	46
185	Highly Active PdO/Mn ₃ O ₄ /CeO ₂ Nanocomposites Supported on One Dimensional Halloysite Nanotubes for Photoassisted Thermal Catalytic Methane Combustion. Angewandte Chemie - International Edition, 2021, 60, 18552-18556.	7.2	46
186	Thermal decomposition of alkaline-earth metal hydride and ammonia borane composites. International Journal of Hydrogen Energy, 2010, 35, 12405-12409.	3.8	45
187	Chemical reaction controlled synthesis of Cu2O hollow octahedra and core–shell structures. CrystEngComm, 2013, 15, 10028.	1.3	45
188	A Family of Metal–Organic Frameworks with a New Chair-Conformation Resorcin[4]arene-Based Ligand: Selective Luminescent Sensing of Amine and Aldehyde Vapors, and Solvent-Mediated Structural Transformations. Crystal Growth and Design, 2016, 16, 3244-3255.	1.4	45
189	PEGylated GdF ₃ :Fe Nanoparticles as Multimodal <i>T</i> ₁ / <i>T</i> ₂ -Weighted MRI and X-ray CT Imaging Contrast Agents. ACS Applied Materials & Interfaces, 2017, 9, 20426-20434.	4.0	45
190	CO Oxidation Catalyzed by Two-Dimensional Co ₃ O ₄ /CeO ₂ Nanosheets. ACS Applied Nano Materials, 2019, 2, 5769-5778.	2.4	45
191	Oneâ€Dimensional Fe ₂ P Acts as a Fenton Agent in Response to NIRâ€II Light and Ultrasound for Deep Tumor Synergetic Theranostics. Angewandte Chemie, 2019, 131, 2429-2434.	1.6	44
192	A Family of Capsule-Based Coordination Polymers Constructed from a New Tetrakis(1,2,4-triazol-ylmethyl)resorcin[4]arene Cavitand and Varied Dicarboxylates for Selective Metal-Ion Exchange and Luminescent Properties. Crystal Growth and Design, 2015, 15, 3822-3831.	1.4	43
193	Baclofen for stroke patients with persistent hiccups: a randomized, double-blind, placebo-controlled trial. Trials, 2014, 15, 295.	0.7	42
194	One-step co-precipitation synthesis of novel BiOCl/CeO ₂ composites with enhanced photodegradation of rhodamine B. Inorganic Chemistry Frontiers, 2020, 7, 1345-1361.	3.0	42
195	Molecular Nanocluster with a [Sn4Ga4Zn2Se20]8â^' T3 Supertetrahedral Core. Inorganic Chemistry, 2009, 48, 4628-4630.	1.9	41
196	Tetracarboxylate-based Co(ii), Ni(ii) and Cu(ii) three-dimensional coordination polymers: syntheses, structures and magnetic properties. Dalton Transactions, 2010, 39, 9123.	1.6	41
197	Rhombic dodecahedral Fe3O4: ionic liquid-modulated and microwave-assisted synthesis and their magnetic properties. CrystEngComm, 2011, 13, 6017.	1.3	41
198	Syntheses, Structures, Photoluminescence, and Gas Adsorption of Rare Earth–Organic Frameworks Based on a Flexible Tricarboxylate. Crystal Growth and Design, 2011, 11, 5469-5474.	1.4	41

#	Article	IF	CITATIONS
199	Conjugated Microporous Polymers with Bipolar and Double Redoxâ€Active Centers for Highâ€Performance Dualâ€Ion, Organic Symmetric Battery. Advanced Energy Materials, 2021, 11, 2100381.	10.2	41
200	Lanthanide doped Y6O5F8/YF3 microcrystals: phase-tunable synthesis and bright white upconversion photoluminescence properties. Dalton Transactions, 2010, 39, 9153.	1.6	40
201	Ultrathin gâ€C ₃ N ₄ Nanosheets Coupled with AglO ₃ as Highly Efficient Heterostructured Photocatalysts for Enhanced Visibleâ€Light Photocatalytic Activity. Chemistry - A European Journal, 2015, 21, 17739-17747.	1.7	40
202	Selfâ€Assembled Pd@CeO ₂ /γâ€Al ₂ O ₃ Catalysts with Enhanced Activity for Catalytic Methane Combustion. Small, 2017, 13, 1700941.	5.2	40
203	Dualâ€ S ite Singleâ€Atom Catalysts with High Performance for Threeâ€Way Catalysis. Advanced Materials, 2022, 34, e2201859.	11.1	39
204	Pure and intense orange upconversion luminescence of Eu3+ from the sensitization of Yb3+–Mn2+ dimer in NaY(Lu)F4 nanocrystals. Journal of Materials Chemistry C, 2014, 2, 9004-9011.	2.7	38
205	One-step synthesis of water-soluble hexagonal NaScF4:Yb/Er nanocrystals with intense red emission. Dalton Transactions, 2014, 43, 10202.	1.6	38
206	A bimetallic oxide Fe1.89Mo4.11O7 electrocatalyst with highly efficient hydrogen evolution reaction activity in alkaline and acidic media. Chemical Science, 2018, 9, 5640-5645.	3.7	38
207	Systematic Synthesis and Characterization of Single-Crystal Lanthanide Phenylphosphonate Nanorods. Inorganic Chemistry, 2006, 45, 1201-1207.	1.9	37
208	An ideal detector composed of a 3D Gd-based coordination polymer for DNA and Hg ²⁺ ion. Inorganic Chemistry Frontiers, 2016, 3, 376-380.	3.0	37
209	Syntheses, crystal structures and near-infrared luminescent properties of holmium (Ho) and praseodymium (Pr) ternary complexes. Inorganic Chemistry Communication, 2008, 11, 531-534.	1.8	36
210	Colloidal Nobleâ€Metal and Bimetallic Alloy Nanocrystals: A General Synthetic Method and Their Catalytic Hydrogenation Properties. Chemistry - A European Journal, 2010, 16, 6251-6256.	1.7	36
211	Near-infrared luminescent copolymerized hybrid materials built from tin nanoclusters and PMMA. Nanoscale, 2010, 2, 2096.	2.8	35
212	Acid–Baseâ€Triggered Structural Transformation of a Polyoxometalate Core Inside a Dodecahedraneâ€like Silver Thiolate Shell. Angewandte Chemie, 2016, 128, 3763-3767.	1.6	35
213	A general one-pot strategy for the synthesis of Au@multi-oxide yolk@shell nanospheres with enhanced catalytic performance. Chemical Science, 2018, 9, 7569-7574.	3.7	35
214	Surfactant-free preparation of NiO nanoflowers and their lithium storage properties. CrystEngComm, 2011, 13, 4903.	1.3	34
215	A series of POM/Ag-based hybrids: distinct forms and assembly of [AgxLy] complexes through combinational effects of POM and isomeric ligands. CrystEngComm, 2012, 14, 6452.	1.3	34
216	Metal organic framework derived CoFe@N-doped carbon/reduced graphene sheets for enhanced oxygen evolution reaction. Inorganic Chemistry Frontiers, 2018, 5, 1962-1966.	3.0	34

#	Article	IF	CITATIONS
217	Half-Encapsulated Au Nanorods@CeO ₂ Core@Shell Nanostructures for Near-Infrared Plasmon-Enhanced Catalysis. ACS Applied Nano Materials, 2019, 2, 1516-1524.	2.4	34
218	Prussian blue and its analogues for aqueous energy storage: From fundamentals to advanced devices. Energy Storage Materials, 2022, 50, 618-640.	9.5	34
219	Activation of Ammonia Borane Hybridized with Alkalineâ^'Metal Hydrides: A Low-Temperature and High-Purity Hydrogen Generation Material. Journal of Physical Chemistry C, 2010, 114, 14662-14664.	1.5	33
220	Five three/two-fold interpenetrating architectures from self-assembly of fluorene-2,7-dicarboxylic acid derivatives and d10 metals. CrystEngComm, 2011, 13, 2935.	1.3	33
221	Size-dependent catalytic properties of Au nanoparticles supported on hierarchical nickel silicate nanostructures. Dalton Transactions, 2013, 42, 7888-7893.	1.6	33
222	Fe3O4-nanoparticle-decorated TiO2 nanofiber hierarchical heterostructures with improved lithium-ion battery performance over wide temperature range. Nano Research, 2015, 8, 1659-1668.	5.8	33
223	CeO ₂ â€Encapsulated Hollow Ag–Au Nanocage Hybrid Nanostructures as Highâ€Performance Catalysts for Cascade Reactions. Small, 2019, 15, e1903182.	5.2	33
224	Cancer therapeutic strategies based on metal ions. Chemical Science, 2021, 12, 12234-12247.	3.7	33
225	Selective crystallization with preferred lithium-ion storage capability of inorganic materials. Nanoscale Research Letters, 2012, 7, 149.	3.1	32
226	Two high-connected metal–organic frameworks based on d10-metal clusters: syntheses, structural topologies and luminescent properties. Dalton Transactions, 2013, 42, 8183.	1.6	32
227	Sandwich‣tructured Graphene–Nickel Silicate–Nickel Ternary Composites as Superior Anode Materials for Lithiumâ€ion Batteries. Chemistry - A European Journal, 2015, 21, 9014-9017.	1.7	32
228	Tunable bimetallic Au–Pd@CeO ₂ for semihydrogenation of phenylacetylene by ammonia borane. Nanoscale, 2019, 11, 12932-12937.	2.8	32
229	A redox interaction-engaged strategy for multicomponent nanomaterials. Chemical Society Reviews, 2020, 49, 736-764.	18.7	32
230	Hydrothermal synthesis and upconversion photoluminescence properties of lanthanide doped YF3 sub-microflowers. CrystEngComm, 2010, 12, 3537.	1.3	31
231	New class of Preyssler-lanthanide complexes with modified and extended structures tuned by the lanthanide contraction effect. Dalton Transactions, 2012, 41, 2399.	1.6	31
232	Constructing porous MOF based on the assembly of layer framework and p-sulfonatocalix[4]arene nanocapsule with proton-conductive property. CrystEngComm, 2014, 16, 64-68.	1.3	31
233	In situ assembly of well-dispersed gold nanoparticles on hierarchical double-walled nickel silicate hollow nanofibers as an efficient and reusable hydrogenation catalyst. Chemical Communications, 2014, 50, 5447-5450.	2.2	31
234	Tumor Diagnosis and Therapy Mediated by Metal Phosphorusâ€Based Nanomaterials. Advanced Materials, 2021, 33, e2103936.	11.1	31

#	Article	IF	CITATIONS
235	Near-infrared luminescent mesoporous MCM-41 materials covalently bonded with ternary thulium complexes. Microporous and Mesoporous Materials, 2009, 117, 278-284.	2.2	29
236	Raisin-like rare earth doped gadolinium fluoride nanocrystals: microwave synthesis and magnetic and upconversion luminescent properties. CrystEngComm, 2012, 14, 4266.	1.3	29
237	Facile Synthesis and Thermoelectric Properties of Selfâ€assembled Bi ₂ Te ₃ Oneâ€Dimensional Nanorod Bundles. Chemistry - A European Journal, 2013, 19, 2889-2894.	1.7	29
238	Template-free solvothermal synthesis and enhanced thermoelectric performance of Sb2Te3 nanosheets. Journal of Alloys and Compounds, 2013, 558, 6-10.	2.8	29
239	Four coordination polymers constructed by a novel octacarboxylate functionalized calix[4]arene ligand: syntheses, structures, and photoluminescence property. CrystEngComm, 2014, 16, 9939-9946.	1.3	29
240	Multifunctional nanostructures based on porous silica covered Fe3O4@CeO2–Pt composites: a thermally stable and magnetically-recyclable catalyst system. Chemical Communications, 2014, 50, 7198.	2.2	29
241	Galvanic replacement synthesis of Ag _x Au _{1â^'x} @CeO ₂ (0 ≤ ≤) core@shell nanospheres with greatly enhanced catalytic performance. Chemical Science, 2015, 6, 7015-7019.	3.7	29
242	A New Coâ€P Nanocomposite with Ultrahigh Relaxivity for In Vivo Magnetic Resonance Imagingâ€Guided Tumor Eradication by Chemo/Photothermal Synergistic Therapy. Small, 2018, 14, 1702431.	5.2	29
243	Robust Synthesis of Goldâ€Based Multishell Structures as Plasmonic Catalysts for Selective Hydrogenation of 4â€Nitrostyrene. Angewandte Chemie - International Edition, 2020, 59, 1103-1107.	7.2	29
244	A new perspective of lanthanide metal–organic frameworks: tailoring Dy-BTC nanospheres for rechargeable Li–O ₂ batteries. Nanoscale, 2020, 12, 9524-9532.	2.8	29
245	A Polymerâ€Assisted Spinodal Decomposition Strategy toward Interconnected Porous Sodium Super Ionic Conductorâ€Structured Polyanionâ€Type Materials and Their Application as a Highâ€Power Sodiumâ€Ion Battery Cathode. Advanced Science, 2021, 8, e2004943.	5.6	29
246	Cascade-responsive nanobomb with domino effect for anti-tumor synergistic therapies. National Science Review, 2022, 9, nwab139.	4.6	29
247	Salt-tolerant and low-cost flame-treated aerogel for continuously efficient solar steam generation. Solar Energy, 2021, 227, 303-311.	2.9	29
248	Design and synthesis of near-IR luminescent mesoporous materials covalently linked with tris(8-hydroxyquinolinate)lanthanide(III) complexes. Microporous and Mesoporous Materials, 2008, 115, 535-540.	2.2	28
249	Fabrication and characterization of uniform Fe3O4 octahedral micro-crystals. Materials Letters, 2009, 63, 307-309.	1.3	28
250	Microwave-assisted synthesis of hydrophilic BaYF ₅ :Tb/Ce,Tb green fluorescent colloid nanocrystals. Dalton Transactions, 2011, 40, 142-145.	1.6	28
251	Synthesis of flower-like nickel oxide/nickel silicate nanocomposites and their enhanced electrochemical performance as anode materials for lithium batteries. Materials Letters, 2013, 93, 5-8.	1.3	28
252	Crystallization of Fe3+ in an alkaline aqueous pseudocapacitor system. CrystEngComm, 2014, 16, 6707.	1.3	27

#	Article	IF	CITATIONS
253	Construction of trace silver modified core@shell structured Pt-Ni nanoframe@CeO2 for semihydrogenation of phenylacetylene. Nano Research, 2019, 12, 869-875.	5.8	27
254	Fabrication of a vanadium nitride/N-doped carbon hollow nanosphere composite as an efficient electrode material for asymmetric supercapacitors. Nanoscale Advances, 2020, 2, 3865-3871.	2.2	27
255	Ballâ€Milling Induced Debonding of Surface Atoms from Metal Bulk for Construing Highâ€Performance Dualâ€5ite Singleâ€Atom Catalysts. Angewandte Chemie, 2021, 133, 23338-23342.	1.6	27
256	Reversible Phase Transfer of Luminescent ZnO Quantum Dots between Polar and Nonpolar Media. Chemistry - A European Journal, 2013, 19, 6329-6333.	1.7	26
257	An unusual three-dimensional self-penetrating network derived from cross-linking of two-fold interpenetrating nets via ligand-unsupported Ag–Ag bonds: synthesis, structure, luminescence, and theoretical study. New Journal of Chemistry, 2012, 36, 877.	1.4	25
258	A Polymerâ€Oriented Selfâ€Assembly Strategy toward Mesoporous Metal Oxides with Ultrahigh Surface Areas. Advanced Science, 2019, 6, 1801543.	5.6	25
259	Ternary lanthanide (Er3+, Nd3+, Yb3+, Sm3+, Pr3+) complex-functionalized mesoporous SBA-15 materials that emit in the near-infrared range. Journal of Photochemistry and Photobiology A: Chemistry, 2008, 199, 57-63.	2.0	24
260	Constructing channel structures based on the assembly of p-sulfonatocalix[4]arene nanocapsules and [M(bpdo)3]2+(M = Cu, Zn). Chemical Communications, 2008, , 4918.	2.2	24
261	Employing tripodal carboxylate ligand to construct Co(ii) coordination networks modulated by N-donor ligands: syntheses, structures and magnetic properties. Dalton Transactions, 2013, 42, 13231.	1.6	24
262	Near-infrared photoluminescent flowerlike α-In2Se3 nanostructures from a solvothermal treatment. Chemical Engineering Journal, 2013, 225, 474-480.	6.6	24
263	Hopper-like framework growth evolution in a cubic system: a case study of Cu ₂ O. Journal of Applied Crystallography, 2013, 46, 1603-1609.	1.9	24
264	A Bipolar and Selfâ€Polymerized Phthalocyanine Complex for Fast and Tunable Energy Storage in Dualâ€Ion Batteries. Angewandte Chemie, 2019, 131, 10310-10314.	1.6	24
265	Pt nanohelices with highly ordered horizontal pore channels as enhanced photothermal materials. Chemical Science, 2015, 6, 6420-6424.	3.7	23
266	Tin Diselenide Molecular Precursor for Solutionâ€Processable Thermoelectric Materials. Angewandte Chemie - International Edition, 2018, 57, 17063-17068.	7.2	23
267	Constructing radially oriented macroporous spheres with central cavities as ultrastable lithium-ion battery anodes. Energy Storage Materials, 2019, 17, 242-252.	9.5	23
268	Specific Core–Satellite Nanocarriers for Enhanced Intracellular ROS Generation and Synergistic Photodynamic Therapy. ACS Applied Materials & Interfaces, 2020, 12, 5403-5412.	4.0	23
269	A Singleâ€Atom Manipulation Approach for Synthesis of Atomically Mixed Nanoalloys as Efficient Catalysts. Angewandte Chemie - International Edition, 2020, 59, 13568-13574.	7.2	23
270	Synthesis, characterization, and near-infrared luminescent properties of the ternary thulium complex covalently bonded to mesoporous MCM-41. Journal of Solid State Chemistry, 2009, 182, 435-441.	1.4	22

#	Article	IF	CITATIONS
271	Self-Assembled Growth of AgIn(MoO4)2 Submicroplates into Hierarchical Structures and Their Near-Infrared Luminescent Properties. Crystal Growth and Design, 2009, 9, 848-852.	1.4	22
272	Water-soluble Au–CeO2 hybrid nanosheets with high catalytic activity and recyclability. Dalton Transactions, 2012, 41, 7193.	1.6	22
273	Phase-tunable synthesis and upconversion photoluminescence of rare-earth-doped sodium scandium fluoride nanocrystals. CrystEngComm, 2013, 15, 6901.	1.3	22
274	A chelation-induced cooperative self-assembly methodology for the synthesis of mesoporous metal hydroxide and oxide nanospheres. Nanoscale, 2018, 10, 5731-5737.	2.8	21
275	Luminescent Lanthanide Metal–Organic Frameworks. Structure and Bonding, 2014, , 109-144.	1.0	20
276	S,N co-doped carbon nanotubes decorated with ultrathin molybdenum disulfide nanosheets with highly electrochemical performance. Nanoscale, 2017, 9, 6346-6352.	2.8	20
277	Multistimuli-Responsive Polymeric Vesicles for Accelerated Drug Release in Chemo-photothermal Therapy. ACS Biomaterials Science and Engineering, 2020, 6, 5012-5023.	2.6	20
278	Optical fiber sensor based on upconversion nanoparticles for internal temperature monitoring of Li-ion batteries. Journal of Materials Chemistry C, 2021, 9, 14757-14765.	2.7	20
279	Selfâ€Assembly of <i>p</i> ‣ulfonatocalix[4]arene and a Ag–hmt Coordination Polymer into a Porous Structure. European Journal of Inorganic Chemistry, 2008, 2008, 1756-1759.	1.0	19
280	Synthesis, characterization and optical property of flower-like indium tin sulfide nanostructures. Dalton Transactions, 2009, , 1620.	1.6	19
281	Three three-dimensional anionic metal–organic frameworks with (4,8)-connected alb topology constructed from a semi-rigid ligand and polynuclear metal clusters. CrystEngComm, 2011, 13, 6057.	1.3	19
282	Three unprecedented open frameworks based on a pyridyl-carboxylate: synthesis, structures and properties. CrystEngComm, 2012, 14, 1681-1686.	1.3	19
283	Spin canting magnetization in a 3D Cu(ii) complex based on molybdate oxide cluster and 5-triazole isophthalic acid. Dalton Transactions, 2012, 41, 13267.	1.6	19
284	CeO ₂ â€Based Pd(Pt) Nanoparticles Grafted onto Fe ₃ O ₄ /Graphene: A General Selfâ€Assembly Approach To Fabricate Highly Efficient Catalysts with Magnetic Recyclable Capability. Chemistry - A European Journal, 2013, 19, 5169-5173.	1.7	19
285	Facile Synthesis of Hierarchical Magnesium Silicate Hollow Nanofibers Assembled by Nanosheets as an Efficient Adsorbent. ChemPlusChem, 2015, 80, 544-548.	1.3	19
286	Nanoporous Carbon-Coated Bimetallic Phosphides for Efficient Electrochemical Water Splitting. Crystal Growth and Design, 2018, 18, 3404-3410.	1.4	19
287	Ligand-Assisted Coordinative Self-Assembly Method to Synthesize Mesoporous Zn _{<i>x</i>} Cd _{1–<i>x</i>} S Nanospheres with Nano-Twin-Induced Phase Junction for Enhanced Photocatalytic H ₂ Evolution. Inorganic Chemistry, 2020, 59, 5063-5071.	1.9	19
288	Synthesis and luminescent properties of organic–inorganic hybrid macroporous materials doped with lanthanide (Eu/Tb) complexes. Optical Materials, 2011, 33, 582-585.	1.7	18

#	Article	IF	CITATIONS
289	Luminescent character of mesoporous silica with Er2O3 composite materials. Microporous and Mesoporous Materials, 2013, 170, 113-122.	2.2	18
290	Reduced Grapheneâ€Wrapped MnO ₂ Nanowires Selfâ€Inserted with Co ₃ O ₄ Nanocages: Remarkable Enhanced Performances for Lithiumâ€Ion Anode Applications. Chemistry - A European Journal, 2016, 22, 6876-6880.	1.7	18
291	A Simple Strategy for the Controlled Synthesis of Ultrasmall Hexagonalâ€Phase NaYF ₄ :Yb,Er Upconversion Nanocrystals. ChemPhotoChem, 2017, 1, 369-375.	1.5	18
292	Hydrothermal Synthesis and Characterization of Alkaline-Earth Metal Phenylphosphonate Nanostructures. Crystal Growth and Design, 2007, 7, 895-899.	1.4	17
293	High-Brightness, Broad-Spectrum White Organic Electroluminescent Device Obtained by Designing Light-Emitting Layers as also Carrier Transport Layers. Journal of Physical Chemistry C, 2010, 114, 21723-21727.	1.5	17
294	Clean synthesis of ZnCo2O4@ZnCo-LDHs yolk–shell nanospheres composed of ultra-thin nanosheets with enhanced electrocatalytic properties. Inorganic Chemistry Frontiers, 2019, 6, 220-225.	3.0	17
295	Rational design of active layer configuration with parallel graphene/polyaniline composite films for high-performance supercapacitor electrode. Electrochimica Acta, 2021, 398, 139330.	2.6	17
296	Facile Synthesis and Optical Property of Porous Tin Oxide and Europium-Doped Tin Oxide Nanorods through Thermal Decomposition of the Organotin. Journal of Physical Chemistry C, 2008, 112, 19939-19944.	1.5	16
297	A long-wave optical pH sensor based on red upconversion luminescence of NaGdF ₄ nanotubes. RSC Advances, 2014, 4, 55897-55899.	1.7	16
298	Guests inducing p-sulfonatocalix[4]arenes into nanocapsule and layer structure. Journal of Solid State Chemistry, 2010, 183, 1457-1463.	1.4	15
299	Fabrication and characterization of magnetic mesoporous silica nanospheres covalently bonded with europium complex. Dalton Transactions, 2010, 39, 5166.	1.6	15
300	Fabrication of fluorescent silica–Au hybrid nanostructures for targeted imaging of tumor cells. Dalton Transactions, 2011, 40, 4800.	1.6	15
301	Cobalt and nickel with various morphologies: mineralizer-assisted synthesis, formation mechanism, and magnetic properties. CrystEngComm, 2011, 13, 223-229.	1.3	15
302	Facile Synthesis of Wellâ€Dispersed Silver Nanoparticles on Hierarchical Flowerâ€like Ni ₃ Si ₂ O ₅ (OH) ₄ with a High Catalytic Activity towards 4â€Nitrophenol Reduction. Chemistry - an Asian Journal, 2012, 7, 2955-2961.	1.7	15
303	Single-crystalline CuGeO3 nanorods: Synthesis, characterization and properties. Materials Research Bulletin, 2013, 48, 2654-2660.	2.7	15
304	Core–shell–shell heterostructures of α-NaLuF ₄ :Yb/Er@NaLuF ₄ :Yb@MF ₂ (M = Ca, Sr, Ba) with remarkably enhanced upconversion luminescence. Dalton Transactions, 2016, 45, 11129-11136.	1.6	15
305	Synthesis and characterization of 1D Co/CoFe2O4 composites with tunable morphologies. Chemical Communications, 2008, , 3570.	2.2	14
306	Culn(WO4)2 nanospindles and nanorods: controlled synthesis and host for lanthanide near-infrared luminescence properties. CrystEngComm, 2009, 11, 1987.	1.3	14

#	Article	IF	CITATIONS
307	Controllable Synthesis of NIR-Luminescent ErQ3Nano-/Microstructures through Self-assembly Growth. Crystal Growth and Design, 2010, 10, 4662-4667.	1.4	14
308	Self-assembled 3D flower-like hierarchical Fe3O4/KxMnO2 core–shell architectures and their application for removal of dye pollutants. CrystEngComm, 2012, 14, 2866.	1.3	14
309	Facile synthesis of Pt3Sn/graphene nanocomposites and their catalysis for electro-oxidation of methanol. CrystEngComm, 2012, 14, 7137.	1.3	14
310	Synthesis of hexagonal Zn3(OH)2V2O7·2H2O nanoplates by a hydrothermal approach: Magnetic and photocatalytic properties. Materials Characterization, 2013, 86, 139-145.	1.9	14
311	Preciousâ€Metalâ€Free Nanocatalysts for Highly Efficient Hydrogen Production from Hydrous Hydrazine. Advanced Functional Materials, 2014, 24, 7073-7077.	7.8	14
312	Solid ion transition route to 3D S–N-codoped hollow carbon nanosphere/graphene aerogel as a metal-free handheld nanocatalyst for organic reactions. Nano Research, 2017, 10, 3486-3495.	5.8	14
313	Cobalt nanoparticle–carbon nanoplate as the solar absorber of a wood aerogel evaporator for continuously efficient desalination. Environmental Science: Water Research and Technology, 2021, 8, 151-161.	1.2	14
314	Modulation of the Host–Guest–Guest Interactions in a Metal–Organic Framework for Multiple Anticounterfeiting Applications. Inorganic Chemistry, 2022, 61, 456-463.	1.9	14
315	Self-templated pseudomorphic transformation of ZIF into layered double hydroxides for improved supercapacitive performance. Journal of Colloid and Interface Science, 2022, 622, 309-318.	5.0	14
316	Synthesis, structures and photoluminescence of two Er(III) coordination polymers. Journal of Coordination Chemistry, 2008, 61, 945-955.	0.8	13
317	Cubic spinel In4SnS8: electrical transport properties and electrochemical hydrogen storage properties. Dalton Transactions, 2010, 39, 7021.	1.6	13
318	Efficient blueâ€emitting Ir(III) complexes with phenylâ€methylâ€benzimidazolyl and picolinate ligands: A DFT and timeâ€dependent DFT study. International Journal of Quantum Chemistry, 2013, 113, 1641-1649.	1.0	13
319	Microwave-assisted synthesis of nanoscale Eu(BTC)(H2O)·DMF with tunable luminescence. Science China Chemistry, 2015, 58, 973-978.	4.2	13
320	Hierarchical MoO ₄ ^{2–} Intercalating α-Co(OH) ₂ Nanosheet Assemblies: Green Synthesis and Ultrafast Reconstruction for Boosting Electrochemical Oxygen Evolution. Energy & Fuels, 2021, 35, 2775-2784.	2.5	13
321	Erbium omplexâ€Doped Nearâ€Infrared Luminescent and Magnetic Macroporous Materials. European Journal of Inorganic Chemistry, 2008, 2008, 5513-5518.	1.0	12
322	Self-assembly of guest-induced calix[4]arene nanocapsules into three-dimensional molecular architecture. CrystEngComm, 2008, 10, 658.	1.3	12
323	Uniform In2S3 octahedron-built microspheres: Bioinspired synthesis andÂoptical properties. Solid State Sciences, 2010, 12, 39-44.	1.5	12
324	Bioinspired Green Synthesis of Nanomaterials and their Applications. Current Nanoscience, 2010, 6, 452-468.	0.7	12

SHUYAN SONG

#	Article	IF	CITATIONS
325	Rare-Earth-Doped Bifunctional Alkaline-Earth Metal Fluoride Nanocrystals via a Facile Microwave-Assisted Process. Inorganic Chemistry, 2011, 50, 5327-5329.	1.9	12
326	Co2GeO4 nanoplates and nano-octahedrons from low-temperature controlled synthesis and their magnetic properties. CrystEngComm, 2012, 14, 7306.	1.3	12
327	Synthesis of high-quality l–Ill–VI semiconductor supported Au particles and their catalytic performance. Catalysis Science and Technology, 2012, 2, 488.	2.1	12
328	Synthesis of Fe3O4 nanoflowers by a simple and novel solvothermal process. Materials Letters, 2012, 76, 90-92.	1.3	12
329	An unusual lamellar framework constructed from a tetracarboxylatocalix[4]arene with highly efficient metal-ion exchange. CrystEngComm, 2014, 16, 9520-9527.	1.3	12
330	Cubic KLu ₃ F ₁₀ nanocrystals: Mn ²⁺ dopant-controlled synthesis and upconversion luminescence. Dalton Transactions, 2015, 44, 17286-17292.	1.6	12
331	CeO ₂ supported low-loading Au as an enhanced catalyst for low temperature oxidation of carbon monoxide. CrystEngComm, 2019, 21, 7108-7113.	1.3	12
332	Microwave-assisted synthesis and down- and up-conversion luminescent properties of BaYF5:Ln (Ln =) Tj ETQq0 (0 0 rgBT /C	Verlock 10 ⁻
333	Density functional theory and timeâ€dependent density functional theory study on a series of iridium complexes with tetraphenylimidodiphosphinate ligand. Journal of Physical Organic Chemistry, 2013, 26, 840-848.	0.9	11
334	<scp>l</scp> â€Arginineâ€Triggered Selfâ€Assembly of CeO ₂ Nanosheaths on Palladium Nanoparticles in Water. Angewandte Chemie, 2016, 128, 4618-4622.	1.6	11
335	Self-supported Co3O4wire-penetrated-cage hybrid arrays with enhanced supercapacitance properties. CrystEngComm, 2017, 19, 1459-1463.	1.3	11
336	Thermally Responsive Materials for Bioimaging. Chemistry - an Asian Journal, 2019, 14, 67-75.	1.7	11
337	Layerâ€byâ€Layer Electrodeposition of FTO/TiO 2 /Cu x O/CeO 2 (1 < x < 2) Photocatalysts with High Peroxidaseâ€Like Activity by Greatly Enhanced Singlet Oxygen Generation. Small Methods, 2021, 5, 2100423.	4.6	11
338	Well-defined Sb2S3 microspheres: High-yield synthesis, characterization, their optical and electrochemical hydrogen storage properties. Solid State Sciences, 2011, 13, 1226-1231.	1.5	10
339	Coral-like cobaltous sulfide/N,S-codoped carbon with hierarchical pores as highly efficient noble metal-free electrocatalyst for oxygen reduction reactions. Journal of Alloys and Compounds, 2018, 769, 801-807.	2.8	10
340	Four new water-stable metal-organic frameworks based on diverse metal clusters: Syntheses, structures, and luminescent sensing properties. Journal of Solid State Chemistry, 2019, 269, 386-395.	1.4	10
341	A Bimetallic Nanozyme with Cascade Effect for Synergistic Therapy of Cancer. ChemMedChem, 2022, 17,	1.6	10

³⁴² In situ redox strategy for large-scale fabrication of surfactant-free M-Fe2O3 (M = Pt, Pd, Au) hybrid 3.5 9 nanospheres. Science China Materials, 2016, 59, 191-199.

#	Article	IF	CITATIONS
343	Tin Diselenide Molecular Precursor for Solutionâ€Processable Thermoelectric Materials. Angewandte Chemie, 2018, 130, 17309-17314.	1.6	9
344	Hierarchical Bi ₂ Te ₃ Nanostrings: Green Synthesis and Their Thermoelectric Properties. Chemistry - A European Journal, 2018, 24, 9765-9768.	1.7	9
345	In Situ Construction of Pt–Ni NF@Niâ€MOFâ€74 for Selective Hydrogenation of <i>p</i> â€Nitrostyrene by Ammonia Borane. Chemistry - A European Journal, 2020, 26, 12539-12543.	1.7	9
346	Hollow Zn ₂ GeO ₄ Nanorods Supported on Reduced Graphene Oxides as an Environment-Friendly High-Capacity Anode Material for Lithium Ion Batteries. Science of Advanced Materials, 2013, 5, 523-529.	0.1	9
347	Frequency Specificity of fMRI in Mesial Temporal Lobe Epilepsy. PLoS ONE, 2016, 11, e0157342.	1.1	9
348	Dye-Encapsulated Lanthanide-Based Metal–Organic Frameworks as a Dual-Emission Sensitization Platform for Alachlor Sensing. Inorganic Chemistry, 2022, 61, 9801-9807.	1.9	9
349	Synthesis of Ferrite Nanocrystals Stabilized by Ionicâ€Liquid Molecules through a Thermal Decomposition Route. Chemistry - A European Journal, 2011, 17, 920-924.	1.7	8
350	Supramolecular isomerism, single-crystal to single-crystal transformation induced by release of in situ generated I2 between two supramolecular frameworks. Dalton Transactions, 2013, 42, 5619.	1.6	8
351	Rational design of Nd ³⁺ -sensitized multifunctional nanoparticles with highly dominant red emission. Dalton Transactions, 2016, 45, 8440-8446.	1.6	8
352	Oneâ€Pot Synthesis of Cobaltâ€Doped Pt–Au Alloy Nanoparticles Supported on Ultrathin α o(OH) ₂ Nanosheets and Their Enhanced Performance in the Reduction of <i>p</i> â€Nitrophenol. European Journal of Inorganic Chemistry, 2017, 2017, 146-152.	1.0	8
353	Thermal Decomposition of CdS Nanowires Assisted by ZIF-67 to Induce the Formation of Co ₉ S ₈ -Based Carbon Nanomaterials with High Lithium-Storage Abilities. ACS Applied Energy Materials, 2018, 1, 6242-6249.	2.5	8
354	A Singleâ€Atom Manipulation Approach for Synthesis of Atomically Mixed Nanoalloys as Efficient Catalysts. Angewandte Chemie, 2020, 132, 13670-13676.	1.6	8
355	Rapidly clearable MnCo ₂ O ₄ @PAA as novel nanotheranostic agents for T ₁ /T ₂ bimodal MRI imaging-guided photothermal therapy. Nanoscale, 2021, 13, 16251-16257.	2.8	8
356	Bimetallic catalyst derived from copper cobalt carbonate hydroxides mediated ZIF-67 composite for efficient hydrogenation of 4-nitrophenol. Colloids and Surfaces A: Physicochemical and Engineering Aspects, 2022, 641, 128477.	2.3	8
357	Morphology-controlled synthesis of α-Fe2O3 nanostructures with magnetic property and excellent electrocatalytic activity for H2O2. Solid State Sciences, 2011, 13, 2129-2136.	1.5	7
358	Design and Synthesis of Enantiomerically Pure Chiral Sandwichlike Lamellar Structure: New Explorations from Molecular Building Blocks to Three-Dimensional Morphology. Crystal Growth and Design, 2013, 13, 976-980.	1.4	7
359	Surfactantâ€Guided Synthesis of Porous Pt Shells with Ordered Tangential Channels, Coated on Pd Nanostructures, and Their Enhanced Catalytic Activities. Chemistry - A European Journal, 2018, 24, 15649-15655.	1.7	7
360	Superior Oxygen Evolution Reaction Performance of Co ₃ O ₄ /NiCo ₂ O ₄ /Ni Foam Composite with Hierarchical Structure. ACS Sustainable Chemistry and Engineering, 0, , .	3.2	7

#	Article	IF	CITATIONS
361	Synthesis of hierarchically double-walled Co3O4 hollow nanofibers assembled by nanosheet building units supporting Pt nanoparticles for high-efficient CO oxidation. Materials Letters, 2019, 237, 126-129.	1.3	7
362	Increased solar absorption and promoted photocarrier separation in atomically thin 2D carbon nitride sheets for enhanced visible-light photocatalysis. Chemical Engineering Journal, 2022, 431, 133219.	6.6	7
363	Lithium hydrazide as a potential compound for hydrogen storage. International Journal of Hydrogen Energy, 2012, 37, 5750-5753.	3.8	6
364	Ultra‣mall Noble Metal Ceriaâ€Based Catalytic Materials: From Synthesis to Application. European Journal of Inorganic Chemistry, 2021, 2021, 689-701.	1.0	6
365	Co ₃ O ₄ /CeO ₂ multi-shelled nanospheres derived from self-templated synthesis for efficient catalytic CO oxidation. Dalton Transactions, 2021, 50, 9637-9642.	1.6	6
366	Boosting the Catalytic Performance of CuO _x in CO ₂ Hydrogenation by Incorporating CeO ₂ Promoters. Advanced Sustainable Systems, 2022, 6, .	2.7	6
367	Metal-decorated Ni7S6 composite microflowers: Synthesis, characterization, and application. Materials Research Bulletin, 2014, 53, 199-204.	2.7	5
368	Strongly Coupled Pt–Ni ₂ GeO ₄ Hybrid Nanostructures as Potential Nanocatalysts for CO Oxidation. Chemistry - A European Journal, 2015, 21, 14768-14771.	1.7	5
369	Designed synthesis of multi-functional PEGylated Yb ₂ O ₃ :Gd@SiO ₂ @CeO ₂ islands core@shell nanostructure. Dalton Transactions, 2016, 45, 11522-11527.	1.6	5
370	Dual-functional α-NaYb(Mn)F4:Er3+@NaLuF4 nanocrystals with highly enhanced red upconversion luminescence. RSC Advances, 2016, 6, 33493-33500.	1.7	5
371	Catalytically active Co 3 O 4 hybrid microstructures and their morphology evolution induced by ceria. Materials Research Bulletin, 2017, 96, 2-9.	2.7	5
372	DFT and TDâ€DFT study of iridium complexes with lowâ€colorâ€temperature and lowâ€efficiency rollâ€off properties. Applied Organometallic Chemistry, 2019, 33, e4563.	1.7	5
373	Dualâ€Defects Adjusted Crystalâ€Field Splitting of LaCo _{1â^'<i>x</i>} Ni _{<i>x</i>} O _{3â^'<i>δ</i>} Hollow Multishelled Structures for Efficient Oxygen Evolution. Angewandte Chemie, 2020, 132, 19859-19863.	1.6	5
374	Metal-Organic Frameworks-derived Indium Clusters/Carbon Nanocomposites for Efficient CO2 Electroreduction. Chemical Research in Chinese Universities, 2022, 38, 1287-1291.	1.3	5
375	Synthesis, structure and characterization of new 1D and 2D Ni(II) coordination polymers. Solid State Sciences, 2009, 11, 364-367.	1.5	4
376	Some Strategies for Improving the Photocatalytic Efficiency of Semiconductor Photocatalyst. Reviews in Advanced Sciences and Engineering, 2012, 1, 165-172.	0.6	4
377	Effect of silver nanoparticles on luminescent properties of europium complex in di-ureasil hybrid materials. Journal of Luminescence, 2007, 122-123, 892-895.	1.5	3
378	Syntheses, structures, and magnetic properties of cobalt(II) and nickel(II) coordination polymers based on a V-shaped ligand. Journal of Solid State Chemistry, 2017, 250, 6-13.	1.4	3

#	Article	IF	CITATIONS
379	Robust Synthesis of Goldâ€Based Multishell Structures as Plasmonic Catalysts for Selective Hydrogenation of 4â€Nitrostyrene. Angewandte Chemie, 2020, 132, 1119-1123.	1.6	3
380	Catalytic activity boost of CeO ₂ /Co ₃ O ₄ nanospheres derived from CeCo-glycolate <i>via</i> yolk–shell structural evolution. Inorganic Chemistry Frontiers, 2020, 7, 421-426.	3.0	3
381	[(UO 2)(C 10 H 8 N 2 O 2) 2][HPW 12 O 40]: The First Case of a Uranyl Coordination Network Containing a Kegginâ€∢ype Polyoxometalate. European Journal of Inorganic Chemistry, 2020, 2020, 4577-4580.	1.0	3
382	Carbon anode material formed from template molecules occluded in a magnesium-substituted aluminophosphate. Materials Chemistry and Physics, 2009, 113, 309-313.	2.0	2
383	Synthesis of monodispersed Au–PbS hybrid nanocrystals via a solid–liquid interfacial reaction. CrystEngComm, 2012, 14, 7552.	1.3	2
384	Injection, transport, absorption and phosphorescence properties of a series of platinum (II) complexes with N-heterocyclic carbenes: a DFT and time-dependent DFT study. Journal of Molecular Modeling, 2014, 20, 2437.	0.8	2
385	Photophysical properties and theoretical calculations of Cu(I) dendrimers. Journal of Luminescence, 2014, 148, 103-110.	1.5	2
386	Two new tetrazamacrocycle based Cu(II) complexes with 2D→0D single-crystal to single-crystal transformation. Inorganic Chemistry Communication, 2015, 57, 26-28.	1.8	2
387	Highly Active PdO/Mn 3 O 4 /CeO 2 Nanocomposites Supported on One Dimensional Halloysite Nanotubes for Photoassisted Thermal Catalytic Methane Combustion. Angewandte Chemie, 2021, 133, 18700-18704.	1.6	2
388	Photothermalâ€Driven Highâ€Performance Selective Hydrogenation System Enabled by Delicately Designed IrCo Nanocages. Small, 2022, 18, .	5.2	2
389	Poly[[diaquabis{μ-4-[6-(4-carboxyphenyl)-4,4′-bipyridin-2-yl]benzoato-κ2O:N4′}zinc] dimethylformamide tetrasolvate]. Acta Crystallographica Section E: Structure Reports Online, 2012, 68, m1413-m1413.	0.2	1
390	Green self-redox synthesis of Rh-PPy-RGO ternary nanocomposite with highly increased catalytic performances. Main Group Chemistry, 2017, 16, 199-206.	0.4	1
391	Research progresses of lanthanide sulfides. Scientia Sinica Chimica, 2012, 42, 1337-1355.	0.2	1
392	Hierarchical Gold Nanoflower Syntheses and Surface-Enhanced Raman Scattering Properties Research. Science of Advanced Materials, 2013, 5, 1797-1800.	0.1	1
393	Formation of nanographite using GaPO ₄ â€LTA as template. Chinese Journal of Chemistry, 2004, 22, 1399-1402.	2.6	0
394	Poly[[diaqua(μ-4,4′-bipyridineN,N′-dioxide-κ2O:O′)(μ-terephthalato-κ2O1:O4)cobalt(II)] 4,4′-bipyr monosolvate]. Acta Crystallographica Section E: Structure Reports Online, 2012, 68, m1307-m1307.	idineN,Nâ 0.2	i€²-dioxide
395	Innenrücktitelbild:l-Arginine-Triggered Self-Assembly of CeO2Nanosheaths on Palladium Nanoparticles in Water (Angew. Chem. 14/2016). Angewandte Chemie, 2016, 128, 4687-4687.	1.6	0
396	Efficient White Electroluminescent Device with Stable Emission Spectrum. Acta Chimica Sinica, 2012,	0.5	0

396 70, 1904.

#	Article	IF	CITATIONS
397	Self-Assembled Nanocomposites and Nanostructures for Environmental and Energy Applications. Crystals, 2022, 12, 274.	1.0	0